Annu. Rev. Mater. Res. 2003. 33:155–68
doi: 10.1146/annurev.matsci.33.072302.093511


# METHANOL-RESISTANT OXYGEN-REDUCTION CATALYSTS FOR DIRECT METHANOL FUEL CELLS

A.K. Shukla and R.K. Raman
*Solid State and Structural Chemistry Unit, Indian Institute of Science, Bangalore-560012, India; email: shukla@sscu.iisc.ernet.in*



**Key Words** transition-metal chalcogenides, transition-metal porphyrins, mixed reactants, cathode selectivity

■ **Abstract** Methanol oxidation in the cathode compartment of the fuel cell, which occurs during the oxygen-reduction reaction on Pt-based cathodes, constitutes a significant performance loss in the direct methanol fuel cells. Over the past decade, four types of methanol-resistant oxygen-reduction catalysts have been developed to circumvent this problem. Among these, transition-metal chalcogenides, and in particular RuSe, have shown effective selectivity to oxygen-reduction reaction in the presence of methanol. These catalysts not only can enhance the performance of the conventional direct methanol fuel cells but also could provide a route to develop mixed-reactants direct methanol fuel cells, which could be highly cost-effective in comparison with the conventional direct methanol fuel cells. This article is a brief update on the preparation, characterization, and implications of methanol-resistant oxygen-reduction catalysts.

## INTRODUCTION

Fuel cells convert the chemical energy of a fuel directly into electricity, and because fuel cells operate without a thermal cycle, they offer a quantum jump in the energy-conversion efficiency. Fuel cells also require no emission-control devices as are necessary in conventional energy-conversion devices (1–3). The six generic fuel cells in various stages of development are (*a*) phosphoric acid fuel cells (PAFCs), (*b*) alkaline fuel cells (AFCs), (*c*) polymer electrolyte fuel cells (PEFCs), (*d*) molten carbonate fuel cells (MCFCs), (*e*) solid oxide fuel cells (SOFCs), and (*f*) direct methanol fuel cells (DMFCs). Among these, the polymer electrolyte hydrogen/air and direct methanol fuel cells are most promising systems for portable and residential power applications (4). Although the power efficiencies of polymer electrolyte hydrogen/air fuel cells continue to show steady improvements, problems remain with the use of hydrogen as the active fuel because this hydrogen must be obtained by in situ reformation of solid or liquid hydrocarbons (petroleum, coal, methanol) or be pre-purified and stored as pressurized gas (or in the form of an admixture with a metal alloy, carbon or some other adsorbent). In all cases, either a considerable weight penalty or increased engineering complexity add to the cost.

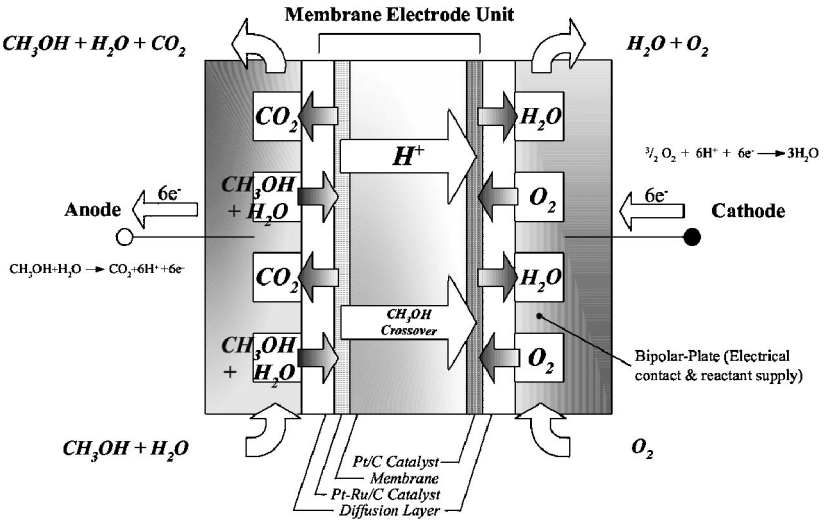


**Figure 1** Schematic diagram of a direct methanol fuel cell.

The direct methanol fuel cell (DMFC), shown schematically in Figure 1 (A.K. Shukla, C.L. Jackson & K. Scott, unpublished information), oxidizes liquid methanol at the anode according to the reaction

$$CH_3OH + H_2O \rightarrow CO_2 + 6H^+ + 6e^- \ (E_a = 0.02\,V \text{ versus SHE}), \qquad 1.$$

where SHE stands for the standard hydrogen electrode.

Consequently, DMFCs do not require a reformer, making them simpler to operate, and thus they are among the higher potential fuel cell options. The cathode reaction in a DMFC proceeds as

$$3/2O_2 + 6H^+ + 6e^- \rightarrow 3H_2O \qquad (E_c = 1.23\,V \text{ versus SHE}). \qquad 2.$$

Accordingly, the net cell reaction in a DMFC is

$$CH_3OH + 3/2O_2 \rightarrow CO_2 + 2H_2O \qquad (E_{cell} = 1.21\,V). \qquad 3.$$

Methanol possesses a number of advantages as a fuel; it is a liquid and therefore can be easily transported and stored and can be dispensed within the current fuel network. Methanol is cheap and plentiful, and the only products of combustion are $CO_2$ and water. Because DMFCs operate at temperatures below 150°C, there is no production of $NO_x$. Above all, the use of methanol directly as an electrochemically active fuel highly simplifies the engineering problems at the front end of the cell, driving down complexity and hence cost.

However, owing to the high degree of irreversibility of the oxygen-reduction reaction, even under open-circuit conditions, the overpotential at the oxygen electrode in a polymer electrolyte hydrogen/air fuel cell is about 0.2 V. This

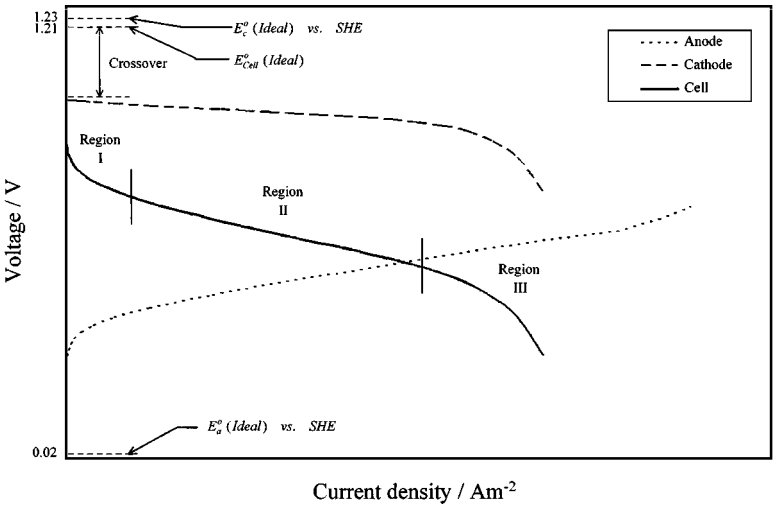


**Figure 2** Polarization curves for a DMFC and its constituent electrodes.



represents a loss of about 20% from the theoretical maximum efficiency for the polymer electrolyte hydrogen/air fuel cells. The situation is even worse with the DMFCs. The thermodynamic potential for a DMFC is 1.21 V, which is only 20 mV less than that for the polymer electrolyte hydrogen/air fuel cells. But in a DMFC, both the methanol oxidation and oxygen-reduction reactions are highly irreversible and thus there is a loss of about 0.2 V at the anode under open-circuit conditions, and an enhanced loss of about 0.1 V at the oxygen electrode because of the crossover of methanol from the anode to the cathode (Figure 2) (5; G. Murgia, L. Pisani, A.K. Shukla & K. Scott, unpublished information). Experimentally, this problem has been tackled by seeking alternative oxygen-reduction catalysts and substantially increasing the platinum loading. The latter method clearly increases the cost significantly.

Before we discuss methanol-resistant oxygen-reduction catalysts in depth, it would be helpful to review the mechanism of oxygen-reduction reactions.

## MECHANISM FOR OXYGEN-REDUCTION REACTIONS

The oxygen-reduction reaction can occur by two different reaction pathways (2): (*a*) the direct four-electron pathway and (*b*) the peroxide pathway. The direct four-electron pathway in an alkaline medium proceeds as

$$O_2 + 2H_2O + 4e^- \rightarrow 4OH^- \qquad (E^o = 0.4\,V \text{ versus SHE}),$$

and in acidic medium as

$$O_2 + 4H^+ + 4e^- \rightarrow 2H_2O \qquad (E^o = 1.23\,V \text{ versus SHE}).$$

The peroxide reaction pathway in an alkaline medium proceeds as

$$O_2 + H_2O + 2e^- \rightarrow HO_2^- + OH^- \qquad (E^o = -0.07\,V \text{ versus SHE}),$$

followed by peroxide reduction to $OH^-$ ions as

$$HO_2^- + H_2O + 2e^- \rightarrow 3OH^- \qquad (E^o = 0.87\,V \text{ versus SHE})$$

or by chemical decomposition of peroxide as

$$2HO_2^- \rightarrow 2OH^- + O_2.$$

In the acidic medium, production of dioxygen through the peroxide pathway is possible as follows:

$$O_2 + 2H^+ + 2e^- \rightarrow H_2O_2 \qquad (E^o = 0.67\,V \text{ versus SHE}).$$

This follows as either

$$H_2O_2 + 2H^+ + 2e^- \rightarrow 2H_2O \qquad (E^o = 1.77\,V \text{ versus SHE})$$
$$\text{or} \quad 2H_2O_2 \rightarrow 2H_2O + O_2.$$

The direct four-electron reaction pathway does not involve the peroxide species and hence is more efficient in relation to the peroxide reaction pathway. However, it has been difficult to find catalysts that would facilitate the direct four-electron reaction pathway for dioxygen reduction.

## CATALYSTS FOR THE OXYGEN-REDUCTION REACTION

At present, four classes of oxygen-reduction catalysts are known. The most familiar of these are the noble metals, particularly platinum, which has been extensively investigated as pure metal (6), platinum nanoparticles (7), and platinum metal alloys (6, 8–11), and as polycrystalline and single-crystal surfaces (12–13). Among the binary alloys of transitional metals with platinized carbon, Pt-Co and Pt-Fe alloy catalysts have been reported as potential methanol-resistant oxygen-reduction catalysts (6). A second class of electrocatalysts is made up of the macrocyclic derivatives of a wide range of transition-metal compounds (14). The most well investigated of these are cobalt and iron, and among the ligands studied, porphyrins, tetra-azaanulenes, and dimethyl glyoxime derivatives are well established (15–18).

A third class of catalysts is derived from metallic oxides (19). Many oxides, particularly of the second- and third-row transition elements, show metallic conductivity (20), usually derived from M-O-M bonding rather than direct M-M overlap to maximize *d*-orbital electron density at the Fermi level, and therefore can be fabricated into electrodes without addition of a conducting matrix. In an alkaline solution, for instance, a number of such oxides, including spinel (21), perovskite

(22), and pyrochlore structures (23), show remarkable activity for oxygen reduction, but in acid solutions, the activity declines substantially, and the stability of the oxide phase is also far less. Related to the oxides are members of the fourth class of electrocatalysts, which are based on transition-metal compounds and other non-metallic counter ions derived from the chalcogenides (24–36). The chalcogenides are frequently highly stable, especially in combination with later transition metals, and can be immersed in aqueous acids and held at high-positive potentials without any appreciable degradation. Studies of compounds from this class have only taken place within the past ten years, but it is already clear that their activity toward oxygen reduction is remarkable. The preparatory methods for the above oxygen-reduction catalysts are briefly summarized in the following section.

## PREPARATION OF METHANOL-RESISTANT OXYGEN-REDUCTION CATALYSTS AND THEIR CHARACTERIZATION

If either the particle size of a platinum electrocatalyst for oxygen reduction is very small or the platinum electrocatalyst is amorphous, the methanol chemisorption energy should be lower and the cathode less poisonable (4). Accordingly, various preparatory routes have been proposed to synthesize platinum and platinum-alloy electrocatalysts with finer particle size (37). Among these, the most attractive procedure comes from Bönnemann et al. (38, 39); here the platinum dichloride ($PtCl_2$) is suspended in tetrahydrofuran (THF) and treated with tetra-alkyl ammonium hydro-tri-organoborate, which results in a platinum metal colloid solution with a minimal evolution of hydrogen. This colloidal solution is evaporated to dryness under high vacuum, and the resultant waxy residue is mixed with ether. The colloid is then precipitated by addition of ethanol. The gray-black metal colloidal powder thus obtained has a particle size between 1 and 5 nm. Maillard et al. (40) reported that the mass activity of platinum toward oxygen reduction increases continuously with a decrease in particle size from 4.6 to 2.3 nm, whereas mass activity is roughly independent of size in methanol-free electrolyte when the platinum particle size is less than 3.5 nm. The effects of adding a second metal to platinum have also been investigated. Although both Pt-Co/C and Pt-Fe/C have been reported to be methanol-resistant oxygen-reduction catalysts, Pt-Fe/C has been found to exhibit higher activity than Pt-Co/C as a methanol-resistant oxygen-reduction catalyst. The X-ray diffraction (XRD) patterns for Pt-Fe/C, Pt-Co/C, and Pt/C catalysts are shown in Figure 3*a,b,c*, respectively (R.K. Raman & A.K. Shukla, unpublished information). The XRD patterns for Pt-Fe/C and Pt-Co/C exhibit tetragonal structures (8, 40a, 41–43). The XRD pattern of Pt/C shown in Figure 3*a* could be fitted to a face-centered cubic phase (41).

Iron tetramethoxyphenylporphyrin (FeTMPP) has been reported to be the most active catalyst among transition-metal porphyrins (17, 44). It is prepared by iron insertion into meso-tetramethoxyphenylphorphyrin ($TMPPH_2$). In brief, $TMPPH_2$

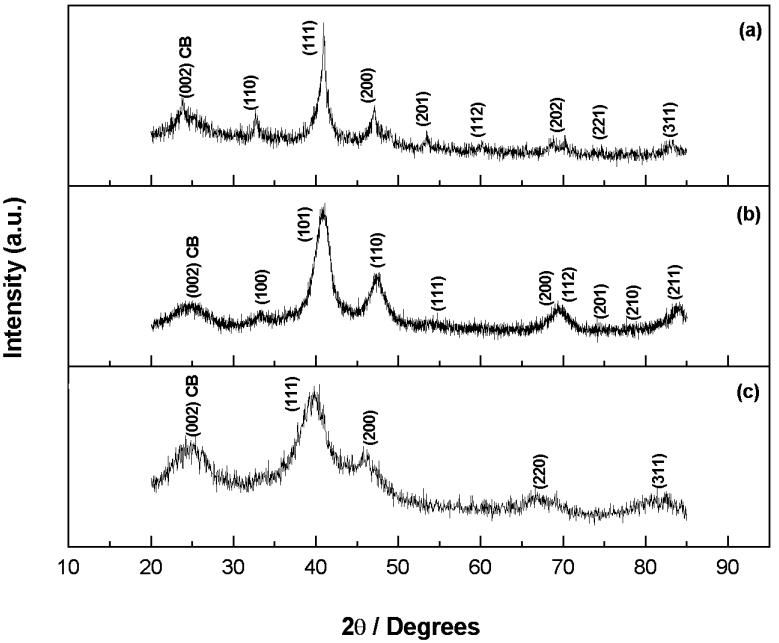


**Figure 3** X-ray powder diffraction pattern for (*a*) Pt-Fe/C, (*b*) Pt-Co/C, and (*c*) Pt/C catalysts.



is synthesized by the reaction of pyrrole with anisaldehyde in propionic acid (45). $TMPPH_2$ thus obtained is purified by column chromatography followed by iron metal insertion with ferric chloride. FeTMPP is typically characterized by absorption spectroscopy and NMR. The characteristic absorption spectrum of FeTMPP in benzene shows absorption maximum ($\lambda_{max}$) in the visible region between 419 and 575 nm. FeTMPP is supported onto a high-surface-area carbon, such as Vulcan XC-72R, and is pyrolyzed at ~700°C in flowing argon (15, 16). In pyrolyzed metal porphyrins, the molecular structure of the catalyst is destroyed during the heat treatment, and therefore the metal complex by default is the precursor of actual active material. It has been proposed that the catalytic site in FeTMPP/C is $N_4$-Fe (17, 18) bound to the carbon support. This site has been labeled as a low-temperature catalytic site (46). The other catalytic site formed at elevated temperatures is not yet fully characterized. However, it is argued that the organic linkages around the iron atom help prevent its oxidation, which is seminal to its catalytic activity (46). Metal oxides are usually prepared by a solid-state reaction of the component oxides (47) and are characterized primarily by powder XRD.

The last category of the catalysts consists mainly of Ru-Mo-S, RuS, and RuSe (27, 33–35). Among these, RuSe exhibits maximum activity as a selective oxygen-reduction catalyst. RuSe is obtained by reacting a mixture of ruthenium

dodecacarbonyl [$Ru_3(CO)_{12}$] with sulfur or selenium at about 140°C, with xylene in nitrogen under refluxing conditions, followed by washing the resultant mass with triethyl ether (33). These catalysts are deposited onto a Vulcan XC-72R carbon for utilization as oxygen-reduction electrodes. Ruthenium chalcogenide has been characterized by powder XRD. The powder XRD pattern for a carbon-supported RuSe (RuSe/C) catalyst is given in Figure 4 (K. Scott, A.K. Shukla, C.L. Jackson & W.R.A. Mueleman, unpublished information). This XRD pattern shows all characteristic peaks due to ruthenium metal, and a broad feature at the diffraction angle of $2\theta \approx 25^\circ$ can be attributed to the (002) plane of hexagonal structure of Vulcan XC-72R. The diffraction peak observed at $2\theta \approx 32^\circ$ is due to the (100)-oriented silicon wafer, which was used as the substrate for catalyst powder. Bron et al. (33) reported that a ruthenium metal, even after refluxing in a selenium-containing solution, shows little change in its XRD pattern. However, RuSe exhibits higher catalytic activity in relation to ruthenium metal. According to Bron et al. (33), the activity enhancement by selenium is related to an interfacial effect due to the binary structure of the catalyst. Energy dispersive analysis by X-rays (EDAX) of the RuSe/C catalyst suggests that the optimum quantity of selenium is ~15 at. % (33). It is noteworthy that the RuSe/C catalyst is different from a metallic-ruthenium surface, and its activity toward oxygen reduction is substantially higher. Because the RuSe/C catalyst is loaded with organic matter made up of carbonyl or carboxylic groups, its high catalytic activity is probably due to an interaction



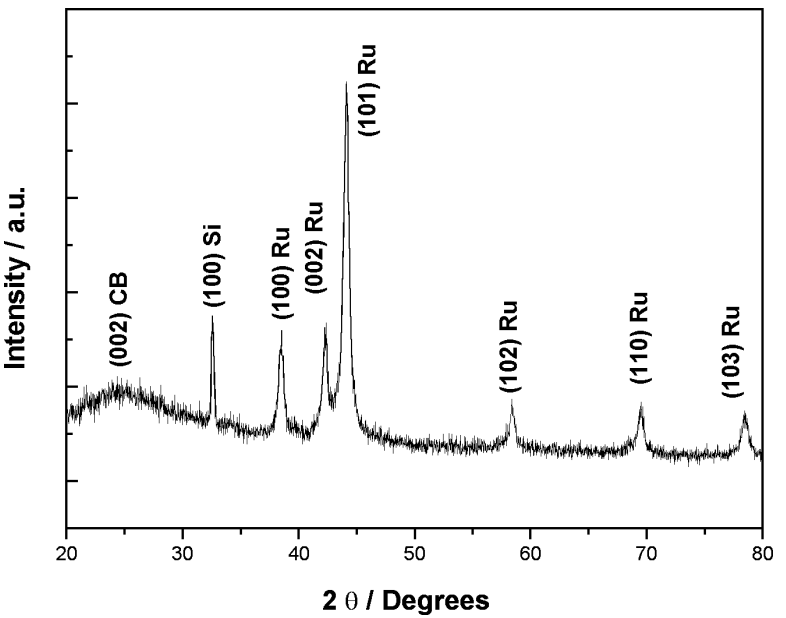


**Figure 4** X-ray powder diffraction pattern for Ru-Se/C catalyst.

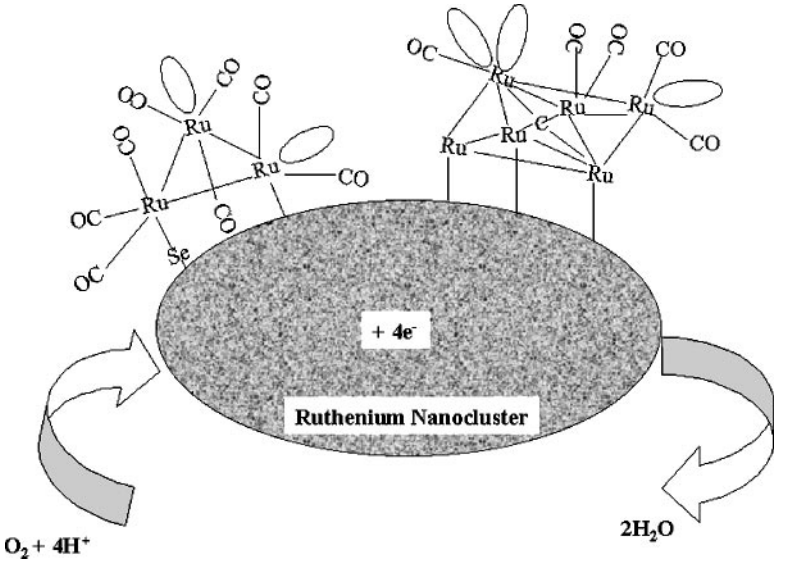


**Figure 5** Mechanism explaining the oxygen-reduction activity of RuSe/C catalyst.

of nanocrystalline ruthenium and carbon ligands. The effect can be twofold: (*a*) Carbon species may stabilize surface ruthenium metal, thus suppressing its oxidation, which otherwise would transform ruthenium particles rapidly into $RuO_2$, and (*b*) carbon species may alter the distribution of interfacial electronic states by forming ruthenium complexes. A schematic description of oxygen reduction on a RuSe/C bistructural catalyst is shown in Figure 5, which depicts catalyst centers consisting of ruthenium clusters with attached carbonyl ligands (48). Because some of the bonds are dangling (unsaturated), an interaction with oxygen can take place depending on the number of ruthenium sites available in the cluster, which act as electron-transfer mediators.

A cyclic voltammetric characterization of Pt/C, Pt-Co/C, and Pt-Fe/C catalysts in aqueous sulfuric acid, both with (Figure 6*b*) and without (Figure 6*a*) methanol, is shown in Figure 6 (R.K. Raman & A.K. Shukla, unpublished information). The data indicate that among Pt/C, Pt-Co/C, and Pt-Fe/C catalysts, methanol oxidation reaction is least favored on the Pt-Fe/C catalyst. Therefore, Pt-Fe/C appears to be a potential selective oxygen-reduction catalyst. Pt-Fe/C has also been reported to be a potential CO-oxidation catalyst (49). The cyclic voltammetric data for FeTMPP/C in aqueous sulfuric acid, with and without methanol, are shown in Figure 6*c*. These data show the methanol resistance of the catalyst toward the oxygen-reduction reaction. The cyclic voltammetric data for RuSe/C in aqueous sulfuric acid, with and without methanol, are given in Figure 6*d*. Here the data depict complete absence of methanol oxidation on the Ru-Se/C surface.

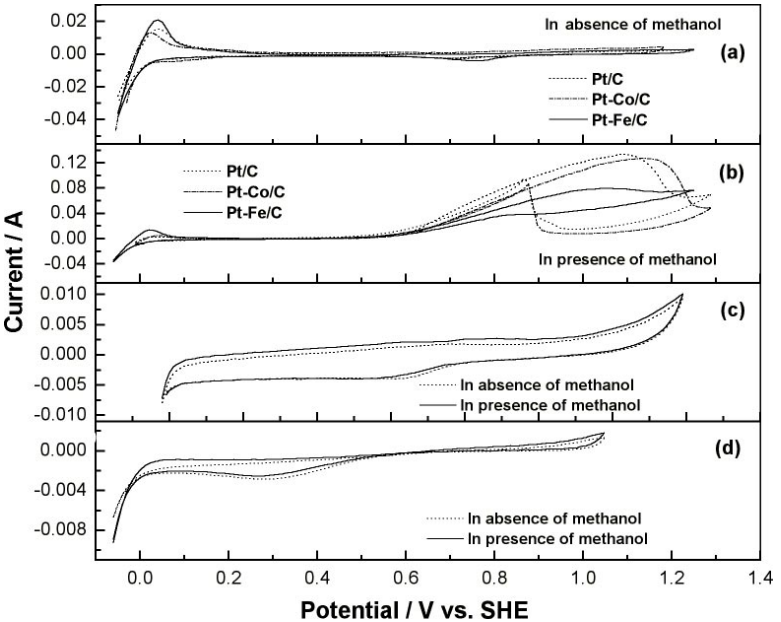


**Figure 6** Cycling voltammograms in aqueous sulfuric acid for (*a*) Pt/C, Pt-Fe/C, and Pt-Co/C without methanol and (*b*) with methanol; (*c*) Fe-TMPP/C catalyst with and without methanol; and (*d*) RuSe/C with and without methanol.

Accordingly, RuSe/C would be an effective selective catalyst for the oxygen-reduction reaction.

## IMPLICATIONS OF METHANOL-RESISTANT OXYGEN-REDUCTION CATALYSTS IN DIRECT METHANOL FUEL CELLS

The development of methanol-resistant oxygen-reduction catalysts would undoubtedly enhance both the cell performance and operational life of DMFCs, as the losses at the cathode due to crossover of methanol could be substantially mitigated. But further innovations in finding cost-effective DMFCs would be mandatory for their commercial realization. A step in this direction appears to be the development of mixed-reactants DMFCs (50–52), which rely on the selectivity of anode and cathode electrocatalysts to separate electrochemical oxidation of the methanol fuel and reduction of oxygen without the need to physically separate the fuel and oxidant. (Such a mixed-reactants DMFC is shown schematically in Figure 7.) Accordingly, in mixed-reactants DMFCs, methanol fuel and oxidant oxygen are mixed together before feeding to the fuel cell. In such a mixed-reactants DMFC,

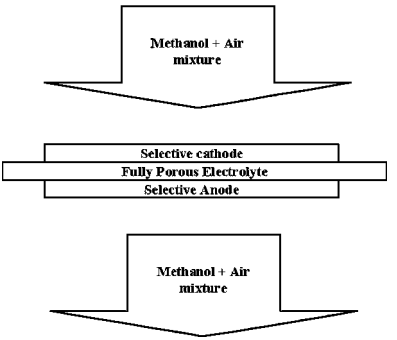


**Figure 7** Schematic description of the mixed-reactants direct methanol fuel cell.



there would be no need for gas-tight structure within the stack, thus providing relaxation for sealing of reactant/product delivery structures (51).

In mixed-reactants DMFCs, cathode selectivity is paramount and is accomplished by using oxygen-reduction catalysts that, in addition to being tolerant to methanol, do not oxidize it (15, 16, 24–35, 53–57). The performance characteristics of certain mixed-reactants DMFCs, employing various methanol-resistant oxygen-reduction catalysts at the cathode and a Pt-Ru/C catalyst at the anode, are shown in Figures 8 and 9 (K. Scott, A.K. Shukla, C.L. Jackson & W. Mueleman, unpublished information). The performance curves at 90°C for the mixed-reactants DMFCs employing 1 mg/cm$^2$ of FeTMPP/C, CoTMPP/C, FeCoTMPP/C, and RuSe/C at the cathode are shown in Figure 8. Among these, the best performance with a maximum power output of ∼30 mW/cm$^2$ is observed for the DMFC employing 1 mg/cm$^2$ of a RuSe/C catalyst at the cathode. The performance curves at 90°C for the mixed-reactants DMFCs employing varying amounts of RuSe/C at the cathode are shown in Figure 9. It is found that the best performance at the maximum output power of about 50 mW/cm$^2$ is obtained for the mixed-reactants DMFCs with the RuSe/C loading of 2.5 mg/cm$^2$ (operating the mixed-reactants DMFC with methanol plus oxygen). A maximum output power of ∼20 mW/cm$^2$ is obtained when operating the cell with methanol plus air.

The cathode polarization curves for oxygen reduction using Pt/C, Pt-Co/C, and Pt-Fe/C catalysts obtained by oxidizing hydrogen at the anode, which also acts as the reference electrode, are shown in Figure 10*a*. These data show superior performance for the Pt/C cathode. But as the methanol passed over the anode, a lower cell performance was found for the cell employing the Pt/C catalyst in relation to both Pt-Co/C and Pt-Fe/C cathodes (Figure 10*c*). This clearly reflects the poisoning of the Pt/C cathode by methanol crossover from anode to cathode. The anode performance was similar for all the cells tested, as shown in Figure 10*b*. The Pt-Co/C catalyst exhibits a performance better than that of the Pt/C catalyst but is inferior to the Pt-Fe/C catalyst (R.K. Raman & A.K. Shukla, unpublished information). These data clearly suggest Pt-Fe/C to be an effective selective

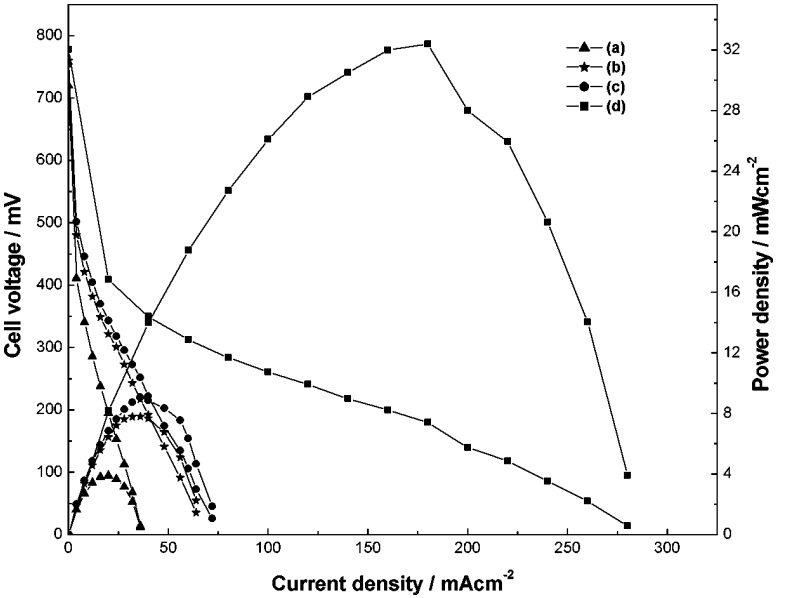


**Figure 8** Performance data for mixed-reactants DMFCs with Pt-Ru/C anode and cathodes containing (*a*) CoTMPP/C, (*b*) FeCoTMPP/C, (*c*) FeTMPP/C, and (*d*) RuSe/C catalysts.

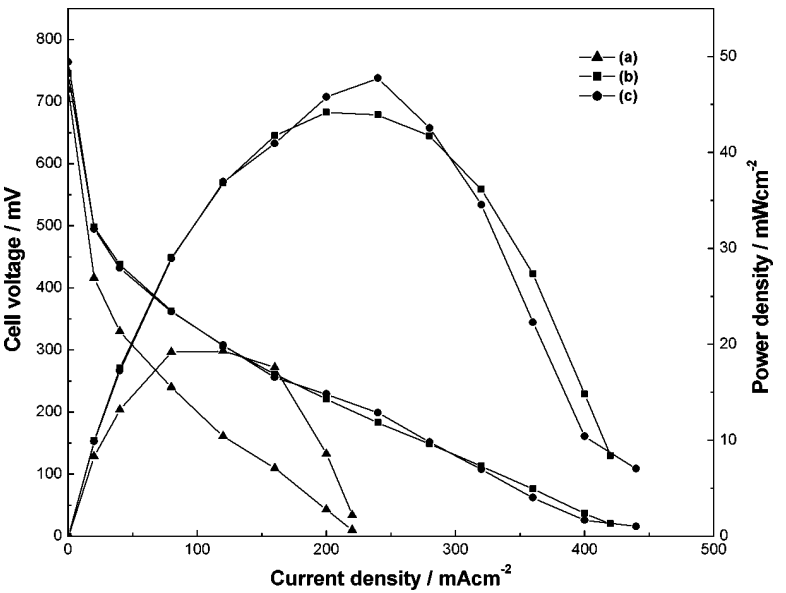


**Figure 9** Performance data for mixed-reactants DMFCs with Pt-Ru/C anode and cathodes with (*a*) 1 mg/cm$^2$, (*b*) 2 mg/cm$^2$, and (*c*) 2.5 mg/cm$^2$ of RuSe/C.

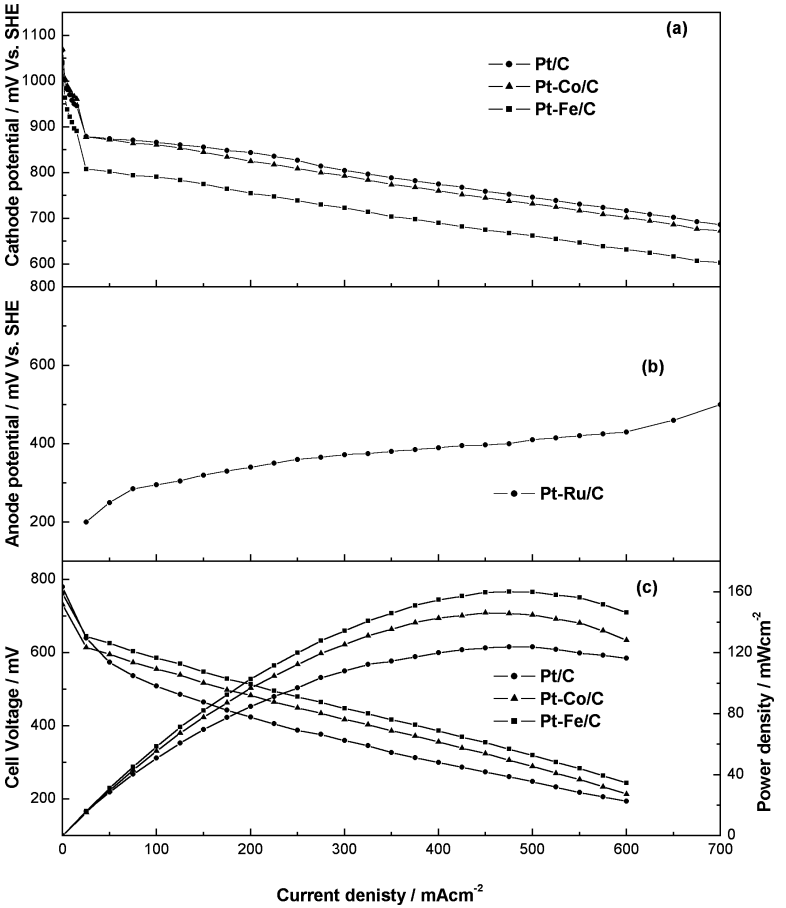


**Figure 10** (*a*) Cathode polarization data for Pt/C, Pt-Co/C, and Pt-Fe/C with 1.37 mg/cm$^2$ Pt loading; (*b*) anode polarization data for Pt-Ru/C using 2.5 mg/cm$^2$ Pt loading; and (*c*) DMFC performance data with PtRu/C anode and cathodes with Pt-Fe/C, Pt-Co/C, and Pt/C.

oxygen-reduction catalyst and conform with the cyclic voltammetry data on Pt/C, Pt-Co/C, and Pt-Fe/C presented in Figure 6.

## CONCLUSIONS

During the past decade, there have been efforts to develop methanol-resistant oxygen-reduction catalysts to mitigate the performance losses in the direct methanol fuel cells that occur through methanol crossover to the cathode. Among the various types of methanol-resistant oxygen-reduction catalysts studied so far, RuSe

has been found to be most effective. The development of an effective methanol-resistant oxygen-reduction catalyst would not only enhance the performance of the conventional direct methanol fuel cells but would also promote the development of cost-effective mixed-reactants DMFCs.

## ACKNOWLEDGMENTS

The senior author (AKS) expresses his gratitude to all of his collaborators in the field of direct methanol fuel cells for their invaluable contribution to this research activity. In particular, he is highly indebted to Professor J.B. Goodenough (University of Texas at Austin), Professor Andrew Hamnett (Starthclyde University, UK), Dr. Paul Christensen (University of Newcastle, UK), Professor Keith Scott (University of Newcastle, UK), Dr. A.S. Aricò (CNR-TAE, Italy), Dr. V. Antonucci (CNR-TAE, Italy), Dr. G. Murgia (CRS-4, Italy), and Professor S. Srinivasan (Princeton University).





## LITERATURE CITED

1. Larminie J, Dicks A. 2000. *Fuel Cell Systems Explained*. New York: Wiley
2. Kordesch K, Simader G. 1994. *Fuel Cells and Their Applications*. Weinheim: VCH
3. Hamnett A. 1996. *Philos. Trans. R. Soc. London Ser. A* 354:1653–69
4. Aricò AS, Srinivasan S, Antonucci V. 2001. *Fuel Cells* 1:1–29
5. Aricò AS, Shukla AK, Kim H, Park S, Min M, Antonucci V. 2001. *Appl. Surf. Sci.* 172:33–40
6. Marković NM, Schmidt TJ, Stamenković V, Ross PN. 2001. *Fuel Cells* 1:105–16
7. Geines L, Faure R, Durand R. 1998. *Electrochim. Acta* 44:1317
8. Toda T, Igarashi H, Uchida H, Watanabe M. 1999. *J. Electrochem. Soc.* 146:3750–56
9. Toda T, Igarashi H, Watanabe M. 1998. *J. Electrochem. Soc.* 145:4185–88
10. Mukerjee S, Srinivasan S, Soriaga MP, McBreen J. 1995. *J. Electrochem. Soc.* 142: 1409–22
11. Mukerjee S, Srinivasan S, Soriaga MP, McBreen J. 1995. *J. Phys. Chem.* 99: 4577–89
12. Štrbac S, Adžić RR. 1996. *J. Electroanal. Chem.* 403:169–81
13. Štrbac S, Anastasijević NA, Adžić RR. 1994. *Electrochim. Acta* 39:983–90
14. Jasinski R. 1965. *J. Electrochem. Soc.* 112:526–28
15. Sun GQ, Wang JT, Savinell RF. 1998. *J. Appl. Electrochem.* 28:1087–93
16. Gupta S, Tryk D, Zecevic SK, Aldred W, Guo D, Savinell RF. 1998. *J. Appl. Electrochem.* 28:673–82
17. Gojković SLJ, Gupta S, Savinell RF. 1999. *J. Electroanal. Chem.* 462:63–72
18. Kalvelage H, Mecklenburg A, Kunz U, Hoffmann U. 2000. *Chem. Eng. Technol.* 23:803–7
19. Goodenough JB. 1971. *Prog. Solid State Chem.* 5:39
20. Trassatti S, ed. 1981. *Electrodes of Conducting Metallic Oxides*, Part B. Amsterdam: Elsevier
21. Tarasevich MR, Efremov BN. 1981. In *Electrodes of Conducting Metallic Oxides*, Part A, ed. S Trassatti, pp. 221–60. Amsterdam: Elsevier
22. Tamura H, Yoneyama H, Matsumoto Y.

1981. In *Electrodes of Conducting Metallic Oxides*, Part A, ed. S Trassatti, pp. 261–300. Amsterdam: Elsevier
23. Goodenough JB, Shukla AK, Paliterio C, Jamieson KR, Hamnett A, Manoharan R. 1985. *Br. Patent No. 8422546*
24. Trapp V, Christensen P, Hamnett A. 1996. *Faraday Trans.* 92:4311–19
25. Fischer C, Alonso-Vante N, Fiechter S, Tributsch H. 1995. *J. Appl. Electrochem.* 25:1004–8
26. Reeve RW, Christensen PA, Hamnett A, Haydock SA, Roy SC. 1998. *J. Electrochem.* Soc. 145:3463–71
27. Sebastian PJ, Rodriguez FJ, Solorza O, Rivera R. 1999. *J. New Mater. Electrochem. Syst.* 2:115–19
28. Solorza-Feria O, Citalán-Cigarroa S, Rivera-Noriega R, Fernández-Valverde SM. 1999. *Electrochem. Commun.* 1:585–89
29. Durón S, Rivera-Noriega R, Leyva MA, Nkeng P, Poillerat G, Solorza-Feria O. 2000. *J. Solid State Electrochem.* 4:70–74
30. Durón S, Rivera-Noriega R, Poillerat G, Solorza-Feria O. 2001. *J. New Mater. Electrochem. Syst.* 4:17–23
31. Rodriguez FJ, Sebastian PJ. 2000. *Int. J. Hydrogen Energy* 25:243–47
32. Alanso-Vante N, Bogdanoff P, Tributsch H. 2000. *J. Catalysis* 190:240–46
33. Bron M, Bogdanoff P, Fiechter S, Dorbandt I, Hilgendorff M, et al. 2001. *J. Electroanal. Chem.* 500:510–17
34. Le Rhan V, Alonso-Vante N. 2000. *J. New Mater. Electrochem. Syst.* 3:331–36
35. Tributsch H, Bron M, Hilgendorff M, Schulenburg H, Dorbandt I, et al. 2001. *J. Appl. Electrochem.* 31:739–48
36. Alonso-Vante N, Schubert B, Tributsch H. 1989. *Mater. Chem. Phys.* 22:281–307
37. Petrow HG, Allen RJ. 1976. *U.S. Patent No. 3992331*
38. Bönnemann H, Brijoux W. 1991. *Angew. Chem. Int. Ed. Engl.* 30:1312–14
39. Bönnemann H, Britz P, Endruschat U, Mörtel R, et al. 2000. *J. New Mater. Electrochem. Syst.* 3:199–206
40. Maillard F, Martin M, Gloaguen F, Léger J-M. 2002. *Electrochim. Acta* 47:3431–40
40a. Sun S, Murray CB, Weller D, Folks L, Moser A. 2000. *Science* 287:1989–92
41. Shukla AK, Neergat M, Bera P, Jayaram V, Hegde MS. 2001. *J. Electroanal. Chem.* 504:111–19
42. Neergat M, Shukla AK, Gandhi KS. 2001. *J. Appl. Electrochem.* 31:373–78
43. Mukerjee S, Srinivasan S. 1993. *J. Electroanal. Chem.* 357:201–24
44. Chu D, Jiang R. 2001. *U.S. Patent 6245707*
45. Stevens P, Shukla AK, Hamnett A. 1989. *I. Chem. E. Symp. Ser.* 112:141–49
46. Bron M, Fiechter S, Hilgendorff M, Bogdanoff P. 2002. *J. Appl. Electrochem.* 32: 11–16
47. Hagenmuller P. 1972. *Preparative Methods in Solid State Chemistry.* New York: Academic
48. Bogdanoff P, Fiechter S, Tributsch H, Bron M, Dorbandt I, et al. 1999. *Ger. Patent 10035841–A1*
49. Uchida H, Ozuka H, Watanabe M. 2002. *Electrochim. Acta* 47:3629–36
50. Shukla AK, Jackson CL, Scott K, Murgia G. 2002. *J. Power Sources* 4847:1–9
51. Priestnall MA, Kotzeva VP, Fish DJ, Nilsson EM. 2002. *J. Power Sources* 106:21–30
52. Barton SC, Patterson T, Wang E, Fuller TF, West AC. 2001. *J. Power Sources* 96:329–36
53. Popovici S, Leyffer W, Holze R. 1998. *J. Porphyrins Phthalocyanines* 2:249–60
54. Okada T, Yoshida M, Hirose T, Kasuga K, Yu T, et al. 2000. *Electrochim. Acta* 45: 4419–28
55. Sun GQ, Wang J-T, Gupta S, Savinell RF. 2001. *J. Appl. Electrochem.* 31:1025–31
56. Convert P, Coutanceau C, Crouïgneau P, Gloaguen F, Lamy C. 2001. *J. Appl. Electrochem.* 31:945–52
57. Chu D, Jiang R. 2002. *Solid State Ionics* 148:591–99

*Annual Review of Materials Research*
*Volume 33, 2003*

# CONTENTS



## MATERIALS FOR FUEL CELLS



## CURRENT INTEREST